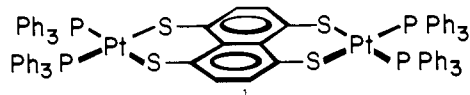


Synthesis, Characterization, and Electrochemistry of a New Platinum "Tetrathiolene" Cluster, $C_{10}H_4S_4Pt_2(P(C_6H_5)_3)_4$: a Novel System with Five Reversible Oxidation States

Sir:

We wish to report here a new "tetrathiolene"¹ platinum dimer, tetrakis(triphenylphosphine)tetrathionaphthalenedi-platinum(II,II) (TTN₂(PPh₃)₄, **1**), which oxidizes in four reversible one-electron steps to give the mono-, di-, tri-, and tetracations, thereby spanning a total of five distinct oxidation states. EPR spectra of the paramagnetic mono- and trications indicate that the electrons are being removed from the predominantly central ligand-based molecular orbitals in these novel oxidation reactions.

The neutral molecule, **1**, was prepared by reacting 1 mol of tetrathionaphthalene (TTN)² with 2 mol (slight excess) of tetrakis(triphenylphosphine)platinum(0) in distilled benzene under an inert atmosphere at room temperature. The orange-red microcrystalline precipitate which formed as the needle-like purple-red TTN crystals gradually disappeared, was filtered, washed with benzene, and recrystallized from methylene chloride/benzene. Elemental analysis indicates the stoichiometry $C_{10}H_4S_4Pt_2(P(C_6H_5)_3)_4$. Infrared spectroscopy of **1** suggests the presence of TTN and PPh₃ ligands. The four bands which are characteristic of coordinated TTN occur at 1524 (w), 1340 (m), 1172 (s), 815 (w) (with a shoulder at 805) cm^{-1} .³ Based on these observations, we propose a planar structure I for **1**.



The significance of **1** lies in its rich redox chemistry. The quadridentate ligand can be considered as a "tetrathiolene" with its electron buffering ability matching that of two "dithiolenes" combined. That is, it can act as, formally, a neutral, mono-, di-, tri-, or a fully reduced tetraanion depending upon the overall bonding environment. Indeed, the cyclic voltammogram (scan rate = 200 mV/s) of a degassed 10^{-3} M solution of **1** in CH_2Cl_2 (using 0.1 M $(n-C_4H_9)_4N^+ClO_4^-$ as supporting electrolyte and Ag|0.01 M $AgNO_3$ in CH_3CN as reference electrode and a platinum bead as working electrode), depicted in Figure 1, revealed four reversible oxidation waves at -0.28 , ~ -0.05 , ~ 0.01 , and 0.31 V.⁴ The first and the fourth waves have peak-to-peak separations of 60 mV which correspond to reversible one-electron oxidations.⁵ The second and the third waves, however, have potentials close to each other (which lie in the range of -0.05 to 0.01 V) such that they merge together to give an apparent single wave at -0.02 V and a peak-to-peak separation of 120 mV. The peak current as well as the i_p^a/i_p^c ratio, when compared with those of the other two waves, strongly suggest that these two waves also correspond to one-electron reversible oxidations.⁵ No apparent reduction wave was observed for **1**. On the other hand, two ill-defined irreversible oxidation waves of **1** at $+1.32$ and $\sim +1.62$ V gave rise to two adsorption reduction waves at 0.16 and 0.38 V on the reversed scan, presumably due to dissociation products at such high positive potentials.

It is important to note that TTN itself oxidizes in two reversible one-electron oxidation steps at $+0.27$ and $+0.65$ V and reduces irreversibly at -1.42 in CH_3CN .² The dramatic shift of the oxidation potentials to more negative values in **1** (i.e., increased ease of oxidation) is consistent with a buildup of negative charge in the TTN ligand upon coordination.

To explore the nature of the molecular orbitals involved in these reversible oxidation reactions, we carried out EPR measurements of the charged species by exhaustively elec-

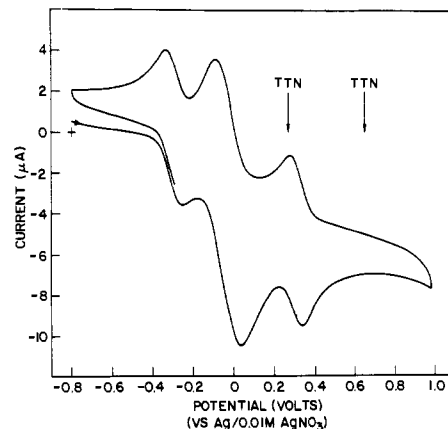


Figure 1. Cyclic voltammogram of a 10^{-3} M solution of $C_{10}H_4S_4Pt_2(P(C_6H_5)_3)_4$ (**1**) in 0.1 M $(n-C_4H_9)_4N^+ClO_4^-$ in CH_2Cl_2 using a scan rate of 200 mV/s, a Pt bead as working electrode, and Ag|0.01 M $AgNO_3$ in CH_3CN as reference electrode.

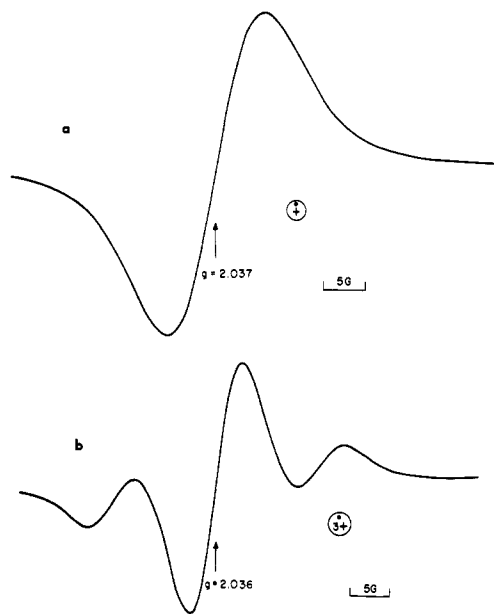


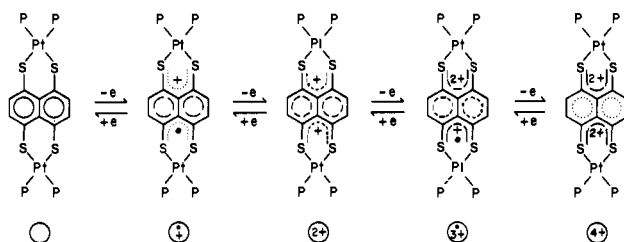
Figure 2. EPR spectra (Varian, X-band, 100-kHz field modulation) of the mono- (a) and trications (b) generated in the microwave cavity at -0.2 and $+0.2$ V, respectively, using 0.1 M $(n-C_4H_9)_4N^+ClO_4^-$ in CH_2Cl_2 as supporting electrolyte and a platinum gauge as working electrode.

trolizing **1** stepwise from -0.6 to $+0.6$ V (cf. Figure 1) in the EPR cavity. Figure 2a and b show the EPR spectra of the paramagnetic mono- and trications, respectively. The neutral, di-, and tetracations give rise to no detectable EPR signal and are presumed to be diamagnetic. The isotropic g value of 2.037 together with no apparent hyperfine splitting observed for the monocation indicate that the spin densities are substantially localized on the TTN ligand.^{6a} The peak-to-peak width of 12.2 G reflects the unresolved small hyperfine splittings due to the TTN hydrogen and the platinum atoms. On the other hand, the trication gives an apparent 1:4:1 triplet EPR signal with $g = 2.036$ and $a_{Pt} = 25.8$ G (i.e., twice the apparent splitting of 12.9 G). This later isotropic hyperfine splitting is consistent with either a mixed valence or nonequivalent platinum formalism for the trication.⁷ Judged from the isotropic $a_{Pt} = 165$ and 82 G observed in $Pt(damn)_2^-$ and $Pt(mnt)_2^-$ complexes,^{6b,c} respectively, we estimate the spin densities on the platinum atom(s) to be ca. 16–32%.

The above observations are in agreement with a molecular orbital calculation performed on $C_{10}H_4S_4Pd_2(PH_3)_4$ using Fenske's nonparameterized method.⁸ The highest occupied orbital of the neutral and the dications are found to be pre-

dominantly TTN in character. These two HOMO's, from which one and two electrons are removed to form the mono- and dications, tri- and tetracations have $a_u(\pi, XZ_-)$ and $b_{3g}(\pi, YZ_+)$ symmetry representations, respectively.^{8c}

We conclude, therefore, that upon successive reversible oxidations, the electrons are being removed from molecular orbitals which are largely localized on the TTN ligand with each square-planar platinum atom maintaining a "formal charge" of +2(d^8) in each species. In other words, the "formal charge" on the TTN ligand decreases from $-4 \rightarrow -3 \rightarrow -2 \rightarrow -1 \rightarrow 0$ as n in $[\text{TTN}Pt_2(\text{PPh}_3)_4]^n$ increases from $0 \rightarrow +1 \rightarrow +2 \rightarrow +3 \rightarrow +4$ (each sulfur atom remains a two-electron donor). The representative limiting valence-bond structures of these five species are summarized below.



We believe that **1** represents the first metal "tetrathiolene" complex which spans five reversible oxidation states. Attempts to synthesize and explore the stereochemical as well as electronic structure of other metal tetrathiolenes are in progress.

Acknowledgments. We thank M. L. Kaplan, F. C. Schilling, and B. E. Prescott for technical assistance.

References and Notes

- (1) For the nomenclature of "metal dithiolenes", see the excellent review by G. N. Schrauzer, *Acc. Chem. Res.*, **2**, 72 (1969).
- (2) For the preparation of TTN ($\text{C}_{10}\text{H}_4\text{S}_4$, dehydrotetrathianaphthazarin, naphtho[1,8-*cd*:4,5-*c'd'*]bis[1,2]dithiole), see F. Wudl, B. Miller, and D. E. Schaefer, *J. Am. Chem. Soc.*, **98**, 252 (1976).
- (3) The corresponding bands in free TTN^{2-} occur at 1540 (s), 1362 (s), 1185 (vs), and 797 (vs) cm^{-1} . The 1172-cm^{-1} band, however, interferes with two very weak bands of triphenylphosphine at 1160 and 1182 cm^{-1} .
- (4) These potentials can be transformed to the corresponding SCE values by adding a factor of 0.285 V.
- (5) See, for example, J. B. Headrig, "Electrochemical Techniques for Inorganic Chemists", Academic Press, New York, N.Y., 1969, Chapter 5.
- (6) (a) A. Y. Giris, Y. S. Sohn, and A. L. Balch, *Inorg. Chem.*, **14**, 2327 (1975); (b) F. C. Senteleber and W. E. Beiger, Jr., *J. Am. Chem. Soc.*, **97**, 5018 (1975); (c) A. Davison, N. Edelstein, R. H. Holm, and A. H. Maki, *ibid.*, **85**, 2029 (1963).
- (7) (a) We expect a 1:4:1 triplet and a 1:8:18:8:1 quintet for the hyperfine interaction(s) with one and two platinum (natural abundance: 33.4% ^{195}Pt with $I = 1/2$) atoms, respectively. (b) Other possibilities include ion-pairing or electron transfer/exchange mechanisms (cf. A. Carrington and A. D. McLachlan, "Introduction to Magnetic Resonance", Harper and Row, New York, N.Y., 1967, pp 215-217).
- (8) (a) B. K. Teo, M. B. Hall, R. F. Fenske, and L. F. Dahl, *Inorg. Chem.*, **14**, 3103 (1975); (b) M. B. Hall and R. F. Fenske, *ibid.*, **11**, 768 (1972). (c) The z and y axes of the metal atoms were chosen to be perpendicular to the molecular plane and bisecting the P-M-P angles, respectively.

Boon-Keng Teo,* F. Wudl, J. H. Marshall, A. Kruger

Bell Laboratories
Murray Hill, New Jersey 07974

Received December 6, 1976

Synthesis and Electronic Properties of the Tetranuclear Trianions $[\text{Fe}_4\text{S}_4(\text{SR})_4]^{3-}$, Analogues of the 4-Fe Active Sites of Reduced Ferredoxins

Sir:

The lower molecular weight iron-sulfur redox proteins¹ contain three recognized types of active sites, $[\text{Fe}(\text{S-Cys})_4]^{-2-}$, $[\text{Fe}_2\text{S}_2(\text{S-Cys})_4]^{2-3-}$, and $[\text{Fe}_4\text{S}_4(\text{S-Cys})_4]^{-2-3-}$, which function in the indicated total oxidation

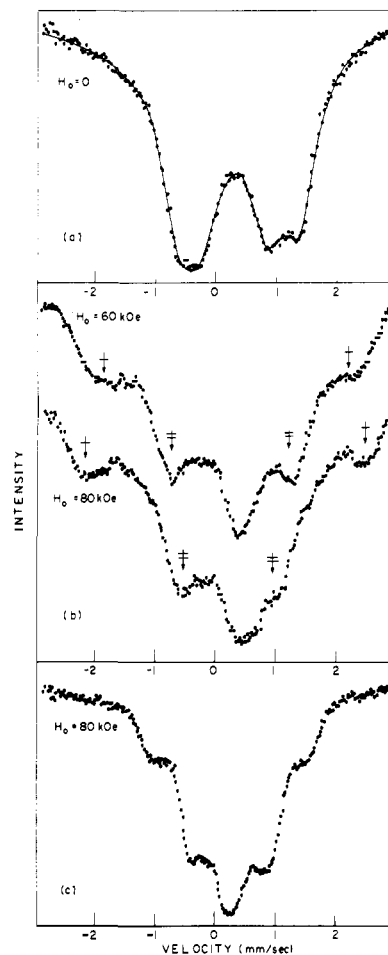


Figure 1. Mössbauer spectra at 4.2 K. (a) $(\text{Et}_4\text{N})_3[\text{Fe}_4\text{S}_4(\text{SPh})_4]$ (I) at $H_0 = 0$. The solid line is a least-squares fit, assuming two sites, Lorentzian line shapes, and line intensities, positions, and widths as free parameters, and gives the $\Delta E_{1,2}$, $\delta_{1,2}$ data in Table I. (b) I at $H_0 = 60$ and 80 kOe; ∇ and \ddagger designate lines moving apart and moving together, respectively, with increasing H_0 . (c) $(\text{Et}_4\text{N})_3[\text{Fe}_4\text{S}_4(\text{SCH}_2\text{Ph})_4]$ (III) at $H_0 = 80$ kOe.

levels. A prime goal of the synthetic analogue approach² to elucidation of key properties of these sites is preparation and isolation in substance of analogues of each of the seven site species. Four such analogues, $[\text{Fe}(\text{SR})_4]^{-2-}$, $[\text{Fe}_2\text{S}_2(\text{SR})_4]^{2-}$, and $[\text{Fe}_4\text{S}_4(\text{SR})_4]^{2-}$, have previously been obtained.^{2,3} Here we report isolation of a fifth synthetic species, $[\text{Fe}_4\text{S}_4(\text{SR})_4]^{3-}$, previously accessible only by generation in solution^{4,5} and analogous to the 4-Fe sites of reduced ferredoxins (Fd_{red}).

Under rigorously anaerobic anhydrous conditions a solution containing $(\text{Et}_4\text{N})_2[\text{Fe}_4\text{S}_4(\text{SPh})_4]^{4-}$ (6.5 mmol), Et_4NCl (6.5 mmol), and sodium acenaphthylenide (8.2 mmol) in 100 mL of freshly distilled hexamethylphosphoramide was stirred for 5 h. Product precipitation with THF followed by recrystallization from acetonitrile-THF afforded pure $(\text{Et}_4\text{N})_3[\text{Fe}_4\text{S}_4(\text{SPh})_4]$ (I) (85%).⁶ Similar procedures but with $(\text{R}_4\text{N})(\text{BPh}_4)$ as common cation source yielded $(\text{Me}_4\text{N})_3[\text{Fe}_4\text{S}_4(\text{SPh})_4]$ (II) and $(\text{Et}_4\text{N})_3[\text{Fe}_4\text{S}_4(\text{SCH}_2\text{Ph})_4]$ (III) (65-85%).⁶ All three salts are intensely oxygen-sensitive,⁷ black crystalline solids. Also obtained by this procedure is the highly crystalline salt $(\text{Et}_3\text{NMe})_3[\text{Fe}_4\text{S}_4(\text{SPh})_4]$, currently under structural investigation.⁸

The isoelectronic relationship $[\text{Fe}_4\text{S}_4(\text{SR})_4]^{3-} \equiv \text{Fd}_{\text{red}}$, previously asserted from generated trianion-protein comparative properties,⁵ is fully confirmed with isolated analogues. Absorption spectra are slightly better resolved and $[\text{Fe}_4\text{S}_4(\text{SCH}_2\text{Ph})_4]^{3-}$ (λ_{max} 358 nm, ϵ 17 600) shows diminished visible absorption vs. $[\text{Fe}_4\text{S}_4(\text{SCH}_2\text{Ph})_4]^{2-}$, characteristic of the $\text{Fd}_{\text{ox}}/\text{Fd}_{\text{red}}$ transition.^{1,9} Axial EPR spectra are